

Magnetohydrodynamic Equilibrium Models for Rotamak Plasmas

I. J. Donnelly, E. K. Rose and J. L. Cook

Australian Atomic Energy Commission,
Lucas Heights Research Laboratories,
Locked Mail Bag No. 1, Menai, N.S.W. 2234.

Abstract

A semi-analytic method is used to solve the Grad-Shafranov equation for a range of compact torus plasma configurations which have ellipsoidal separatrices, zero toroidal magnetic field and pressure P proportional to the square of the poloidal flux function Ψ . The equilibria are compared with the analytic solutions of the Solov'ev model, for which $P \propto \Psi$.

1. Introduction

The rotamak is a compact torus plasma configuration in which the toroidal current is driven by means of an externally generated rotating magnetic field (Hugrass *et al.* 1980). In this paper we ignore confining effects due to the oscillating fields and analyse the magnetohydrodynamic (MHD) equilibrium of the steady-state configuration, which has the form of a field reversed mirror. Also, we confine our analysis to the case of zero toroidal magnetic field, which covers the majority of experiments so far conducted (e.g. Durance and Jones 1986; Durance *et al.* 1987).

To calculate the energy loss processes which determine the plasma temperature, it is necessary to have an equilibrium model which gives the plasma density, temperature and magnetic field profiles. These can be obtained (Storer 1982) using MHD equilibrium codes such as PEST (Grimm *et al.* 1976). However, we wish to survey the dependence of these parameters on the plasma size and shape, on the power input and on the rotating field frequency; such calculations using PEST would be very time consuming. An analytic equilibrium model (Solov'ev 1975), in which the plasma pressure P is proportional to the poloidal flux function Ψ , can be used. However, it predicts a (non-realistic) constant density distribution when coupled with the rotating magnetic field current drive condition that the electron fluid has a rigid-body rotation (Jones and Hugrass 1981). In this paper we develop a semi-analytic method to calculate equilibria for a model with $P \propto \Psi^2$. This model predicts density and temperature profiles which are realistic for warm to hot plasmas. The equilibria are analysed as a function of the plasma size and shape, and comparisons with the Solov'ev equilibria are made. The $P \propto \Psi^2$ equilibria determined here have been used as a basis for the calculation of energy transfer rates in a range of rotamak configurations (Donnelly, Rose and Cook 1987; henceforth referred to as DRC).

In Section 2 the numerical methods used to solve the $P \propto \Psi^2$ equilibrium equations are described. The dependence and scaling of various parameters on the shape and size of the plasma are given in Section 3, and comparisons are made with the Solov'ev model results.

2. Calculation of the Flux Function when $P \propto \Psi^2$

In cylindrical (r, ϕ, z) coordinates the Grad-Shafranov equation for an axisymmetric plasma with zero B_ϕ is

$$r \frac{\partial}{\partial r} \left(\frac{1}{r} \frac{\partial \Psi}{\partial r} \right) + \frac{\partial^2 \Psi}{\partial z^2} = -\mu_0 r^2 \frac{dP}{d\Psi}, \quad (1)$$

where P is the plasma pressure and the flux function Ψ is defined as

$$\Psi(r, z) = \int_0^r B_z(r', z) r' dr'. \quad (2)$$

The condition that $\Psi(r, z)$ is constant defines a flux surface.

We consider the case in which $P \propto \Psi^2$ (henceforth called the Ψ^2 model) and solve equation (1) for a plasma configuration confined inside an ellipsoidal separatrix defined by

$$X^2 + (Z/\zeta)^2 = 1, \quad (3)$$

where ζ determines the ellipticity of the separatrix, R is the separatrix radius at $z = 0$, and where $X = r/R$ and $Z = z/R$. It is convenient to write

$$\Psi(X, Z) = \psi_0 \psi(X, Z), \quad (4)$$

where ψ is normalised to a maximum value of 1, which occurs at the magnetic axis, and ψ_0 is the maximum value of Ψ . For λ defined by

$$P = (2\lambda^2/\mu_0 R^4) \Psi^2, \quad (5)$$

equation (1) becomes

$$X \frac{\partial}{\partial X} \left(\frac{1}{X} \frac{\partial \psi}{\partial X} \right) + \frac{\partial^2 \psi}{\partial Z^2} = -4\lambda^2 X^2 \psi. \quad (6)$$

The solution of this homogeneous partial differential equation is subject to the boundary conditions that $\psi = 0$ on both the separatrix and the z -axis. There is an infinite number of eigenvalues λ for which a solution can be obtained; here we are only interested in the smallest (non-zero) λ , which gives non-negative ψ . As is to be expected, λ is a function of ζ .

Berk *et al.* (1981) have found a solution of equation (6), regular at $X = 0$, which we express in the un-normalised form

$$\psi(X, Z) = F_0(\eta_n, \rho) \cos(k_n Z), \quad (7)$$

where F_0 is the Coulomb wavefunction (Abramowitz and Stegun 1965), $\eta_n = k_n^2/8\lambda$, $\rho = \lambda X^2$ and k_n is an arbitrary constant. To obtain a solution for equation (6) which satisfies the boundary conditions, we use a Fourier expansion in the z direction and write

$$\psi(X, Z) = \sum_{n=0}^N w_n F_0(\eta_n, \rho) \cos(k_n Z), \quad (8)$$

with $k_n = n\pi/M\zeta$. Accurate solutions can be obtained for a range of N and M . In deriving the results presented here we have used $N = 8$, with $M = 4/\zeta$ when $\zeta \leq 4$ and $M = 1$ when $\zeta > 4$. The weighting constants w_n and the eigenvalue λ are determined as follows:

- (i) For any fixed ϕ coordinate, the separatrix is divided into $N+1$ equal segments between $(X = 0, Z = \zeta)$ and $(X = 1, Z = 0)$. We require $\psi = 0$ at the $N+2$ equally spaced end-points of these segments.
- (ii) As equation (6) is linear and homogeneous, the condition $w_0 = 1$ is initially used to determine the amplitude of the solution.
- (iii) A value is assigned to λ , and w_1, \dots, w_N are determined by requiring $\psi = 0$ at all end-points except the first $(X = 0, Z = \zeta)$, where equation (8) guarantees $\psi = 0$, and the last $(X = 1, Z = 0)$.
- (iv) The solution is normalised to a maximum value of 1.
- (v) The value of $\psi(1, 0)$ is calculated.
- (vi) The process (ii)–(v) is iterated on λ until $|\psi(1, 0)| \leq \epsilon$, where ϵ is typically $< 10^{-3}$. These final values of λ and ψ are the solutions for the given ζ .

The sensitivity of λ and ψ to the parameter N has been investigated for $\zeta = 0.25$, 1 and 4. For $\zeta = 1$, a converged eigenvalue (accurate to five figures) and an excellent fit to the separatrix position is obtained for N as low as 4. Comparable accuracies are obtained for $\zeta = 4$ with $N = 6$, and for $\zeta = 0.25$ with $N = 8$. Examination of the case $\zeta = 1$ has shown that the eigenvalues and flux contours predicted with $4 \leq N \leq 15$ are virtually identical. However, when $N > 15$ we have found that errors become evident in the flux contours and the eigenvalues because of numerical problems which arise from the rapid increase of the Coulomb wavefunction with X when η_n is large [$F_0(\eta_n, \rho) \propto X^{1/2} \exp(k_n X)$ when $\eta_n \gg \rho$]. Similar problems prevented us from obtaining converged solutions for $\zeta \leq 0.1$. It appears possible to overcome this difficulty by changing our Coulomb wavefunction routine, but this has not been pursued because the small ζ configurations are not of interest.

Using $k_n = n\pi/M\zeta$ means that the flux function (8) has a periodic length $M\zeta R$ in the z direction. The dependence of the solutions on the parameter M has also been investigated. If $M\zeta$ is large then η_n is small for n small, $F_0(\eta_n, \rho)$ is also independent of n , and the solution fails due to round-off error problems (even though double precision arithmetic is used). If $M\zeta$ is small we encounter the already mentioned problem associated with the calculation of $F_0(\eta_n, \rho)$ for large η_n . Therefore, we have chosen $M = 4/\zeta$ when $\zeta \leq 4$ and $M = 1$ when $\zeta > 4$ (periodicity constraints do not allow $M < 1$). Using $N = 8$ and the above prescription for M gives accurate eigenvalues and flux contours for $0.25 \leq \zeta \leq 4$. Converged eigenvalues have also been obtained for $\zeta = 10$; however, the separatrix contour exhibits indentations in the region $X \approx 0$, $|Z| \approx \zeta$. This arises because, for large ζ , ψ is very small when $|Z| > \zeta^{1/2}$, and small errors in the individual terms in (8) can lead to large percentage

errors in ψ and in the derived fields. Therefore, we restrict the presentation of our results to the range $0.25 \leq \zeta \leq 4$.*

It is interesting to observe that, because the individual terms in equation (8) all satisfy equation (6), it is possible to determine, for an arbitrary λ , a set of w_n so that $\psi = 0$ at $N+1$ equally spaced points around the separatrix from $(X = 0, Z = \zeta)$ to $(X = 1, Z = 0)$ inclusive. However, unless λ is close to an eigenvalue, this results in severe distortions of the flux surfaces, both internally and around the separatrix between the mesh-points.

It is, of course, possible to solve equation (6) using a completely numerical partial differential equation solver, and accurate solutions could (presumably) be obtained for arbitrary ζ . The advantage of the semi-analytic method is that it allows straightforward evaluation of both the volume integrals of the various functions and the derivatives of ψ which are required for the power balance calculations in DRC.

Table 1. Dependence of equilibrium parameters on ζ

ζ	λ	$\frac{\psi_0(\zeta)}{\psi_0(1)}$	$\frac{\psi_0^S(\zeta)}{\psi_0^S(1)}$	$\frac{I_\phi(\zeta)}{I_\phi(1)}$	$\frac{I_\phi^S(\zeta)}{I_\phi^S(1)}$
0.25	7.60	0.50	0.50	0.49	0.50
0.5	4.85	0.78	0.79	0.68	0.62
0.75	4.11	0.93	0.93	0.84	0.81
1.0	3.81	1.00	1.00	1.00	1.00
1.25	3.648	1.04	1.04	1.15	1.20
1.5	3.547	1.07	1.06	1.28	1.41
1.75	3.482	1.09	1.08	1.41	1.63
2.0	3.435	1.11	1.08	1.51	1.84
4.0	3.2825	1.16	1.11	2.22	3.61
$\gg 1$	π	1.21	1.12	—	0.89 ζ

3. Dependence of Equilibrium Fields on ζ

We analyse the equilibrium configuration for $0.25 \leq \zeta \leq 4$ and in the limit of $\zeta = \infty$. In the latter case, the plasma is infinite in the z direction with

$$\psi(X, Z) = \sin(\pi X^2). \quad (9)$$

In Table 1, λ is shown to be a decreasing function of ζ which tends asymptotically to π as ζ tends to ∞ . The listed values of λ contain the number of significant figures that are needed to obtain an accurate fit to the separatrix.

Fig. 1*a* shows the variation of $\psi(X, 0)$ with X for $\zeta = 0.5, 1$ and 2 ; this function is almost independent of ζ . Also shown is the Solov'ev function $\psi^S(X, 0)$ (defined in the Appendix) which is independent of ζ (the superscript S is used to denote the

* In a previous version of this paper we calculated ψ using the prescription $k_n = n\pi/N\zeta$. With $N = 7$ this method gives accurate results when $0.25 \leq \zeta \leq 2$, but it breaks down for $N > 8$ and ζ outside this range because of the numerical problems which arise when k_n is small or large. The Fourier expansion formulation, which we originally discarded because we expected numerical problems associated with large k_n , was re-examined following comments by a referee, and has proven to be superior.

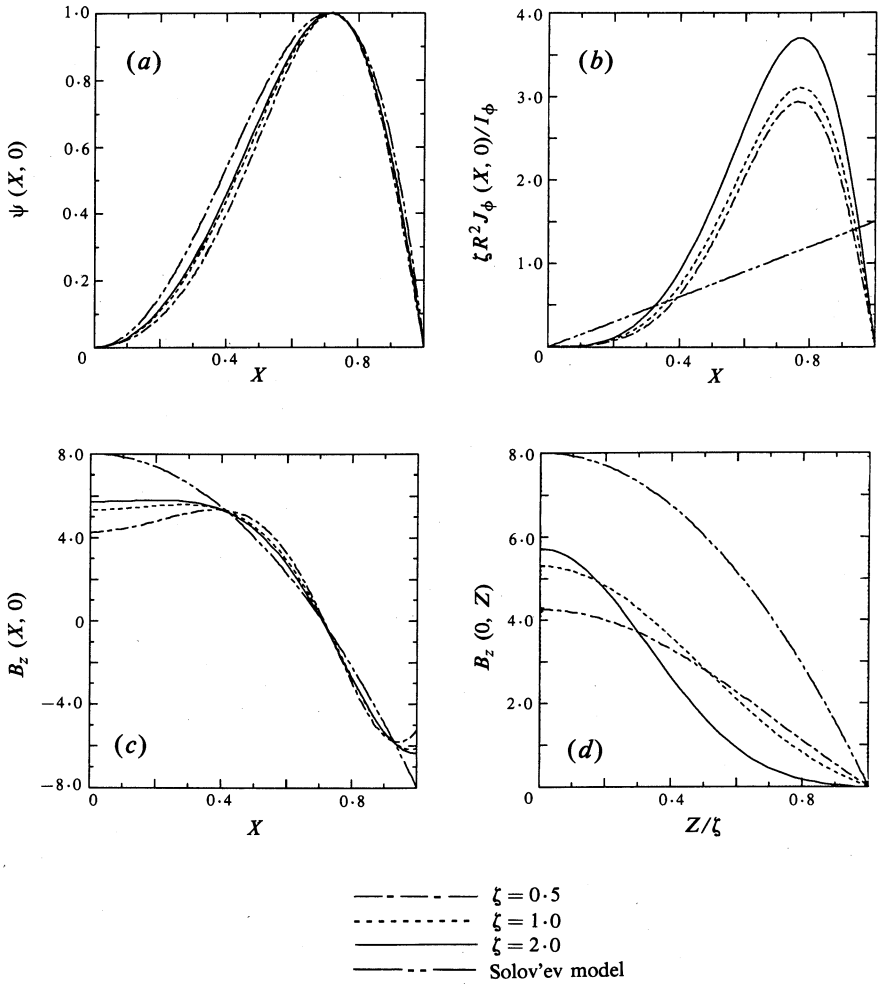


Fig. 1. Profiles of (a) $\psi(X, 0)$, (b) $\zeta R^2 J_\phi(X, 0)/I_\phi$, (c) $B_z(X, 0)$ and (d) $B_z(0, Z)$ for the Ψ^2 model ($\zeta = 0.5, 1.0$ and 2.0) and for the Solov'ev model.

Solov'ev model whenever a comparison with the Ψ^2 model is made). It is apparent that the position of the magnetic axis (where $\psi = 1$) is very close to $X = \sqrt{\frac{1}{2}}$ for all cases.

The magnetic field components are given by

$$B_r = -\frac{\psi_0}{R^2} \frac{1}{X} \frac{\partial \psi}{\partial Z} \quad \text{and} \quad B_z = \frac{\psi_0}{R^2} \frac{1}{X} \frac{\partial \psi}{\partial X}. \quad (10a, b)$$

Fig. 1c shows $B_z(X, 0)$ for $\psi_0/R^2 = 1$ and $\zeta = 0.5, 1$ and 2 ; also shown is B_z^S . For the same parameters, Fig. 1d shows $B_z(0, Z)$ as a function of Z/ζ . From Fig. 1c it is apparent that $B_z(X, 0)$ has a similar dependence on X for both the Ψ^2 and Solov'ev models, except for configurations with small ζ which have $|B_z(X, 0)|$ small at $X \approx 0$ and $X \approx 1$. As ζ becomes smaller than 1, the position of the maximum values of $|B_z(X, 0)|$ moves in from $X = 0$ and 1 towards the magnetic axis.

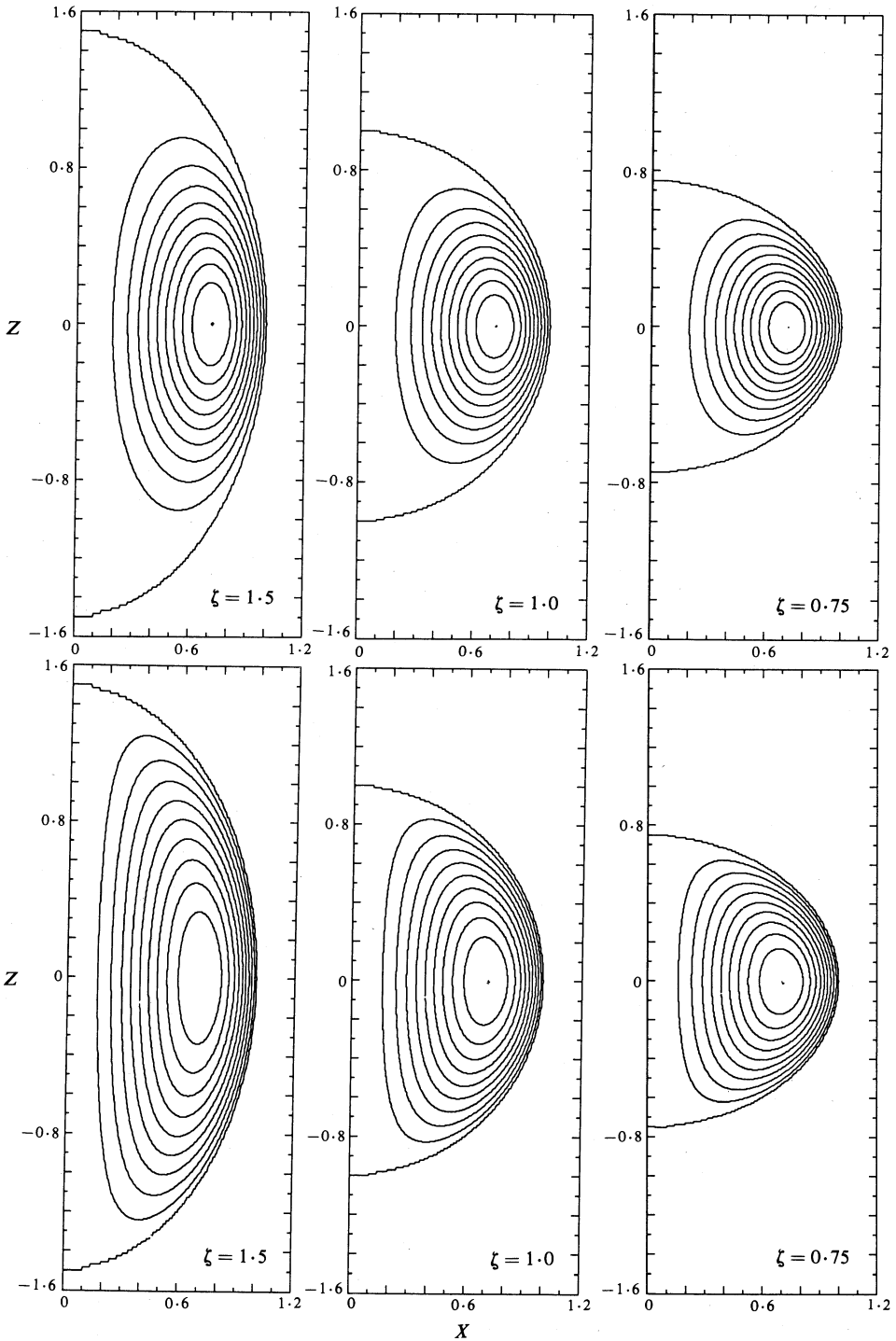


Fig. 2. Comparison of flux surface contours for the Ψ^2 (top) and Solov'ev (bottom) models.

The global form of the magnetic fields can be deduced from the contours of constant ψ which are compared in Fig. 2 for the Ψ^2 and Solov'ev models with $\zeta = 0.75, 1.0$ and 1.5 ; the contour spacing is $\Delta\psi = 0.1$. Note that, relative to the Solov'ev values, the Ψ^2 model contours are less 'D-shaped' and more concentrated around the magnetic axis. For all prolate configurations considered ($1 < \zeta \leq 10$), the $\psi = 0.1$ contour lies in the region $|Z| < \zeta^{1/2}$; this indicates that, in the regions $|Z| > \zeta^{1/2}$, the magnetic field of the Ψ^2 model is much smaller than that of the Solov'ev model, especially near the separatrix. The plots of $B_z(0, Z)$ shown in Fig. 1d illustrate this point.

To see how the magnitude of the flux function depends on ζ , we write

$$P = P_0 \psi^2 \quad (11)$$

and normalise the equilibrium to the same value of P_0 and R for each ζ . Equations (5) and (11) then give

$$\psi_0(\zeta) = (0.5\mu_0 R^4 P_0)^{1/2} / \lambda(\zeta). \quad (12)$$

The ζ dependence of $\psi_0(\zeta)/\psi_0(1)$ [$=\lambda(1)/\lambda(\zeta)$] is compared with the Solov'ev model prediction in Table 1.

The current density is

$$J_\phi = r dP/d\Psi = (4\lambda^2\psi_0/\mu_0 R^3)X\psi, \quad (13)$$

and the total current is

$$I_\phi = (2\lambda^2\psi_0/\pi\mu_0 R)\mathcal{J}_{12}, \quad (14)$$

where

$$\mathcal{J}_{12} = 4\pi \int_0^\zeta dZ \int_0^{X'} X\psi dX, \quad (15)$$

with $X' = \{1 - (Z/\zeta)^2\}^{1/2}$. Fig. 1b shows $\zeta R^2 J_\phi(X, 0)/I_\phi$ for $\zeta = 0.5, 1$ and 2 ; for the Solov'ev model this function is independent of ζ . The current density J_ϕ is obviously more concentrated than J_ϕ^S around the magnetic axis. This leads to the differences in the magnetic field shapes predicted by the two models. From equations (12) and (14), we get

$$I_\phi(\zeta)/I_\phi(1) = \lambda(\zeta)\mathcal{J}_{12}(\zeta)/\lambda(1)\mathcal{J}_{12}(1). \quad (16)$$

The variation of this term with ζ is compared with the Solov'ev model prediction in Table 1.

We note that I_ϕ is proportional to ψ_0 for both the Ψ^2 and Solov'ev models. Therefore, the magnetic field and the current distribution have a fixed shape (which depends only on ζ), and an amplitude which is proportional to the current in the external field coils I_F . Hence the linear increase of I_ϕ with I_F , which has been observed experimentally by Durance *et al.* (1987), implies that the shape of their plasma configuration remains almost constant as I_F is changed, and the plasma pressure increases as I_F^2 .

Equilibrium models determine the plasma pressure distribution, but extra information is needed to obtain the plasma density and temperature profiles. The theory of the rotating magnetic field current drive (Jones and Hugrass 1981) indicates that, given full penetration of the rotating field into the plasma, the electron fluid rotates with a constant angular frequency. When this is combined with expression (13) for the current density, the number density n and the sum of the electron and ion temperatures T are both proportional to ψ . In contrast, the Solov'ev model has $n^S = \text{constant}$ and $T^S \propto \psi^S$. The more realistic expression for n , which is obtained with the Ψ^2 model, is the major reason for our analysis of this model and its use in the power balance studies in DRC.

4. Conclusions

The Grad-Shafranov equation has been solved for the case $P \propto \Psi^2$, subject to the boundary condition that the separatrix is ellipsoidal. The solution method is effective provided the configuration is not too prolate (i.e. provided that $\zeta \leq 4$). The equilibria have been compared with the analytic solution of the Solov'ev model ($P \propto \Psi$). Although there are many similarities, some differences have been identified; in particular, when $\zeta > 1$ the Ψ^2 model has a significantly lower magnetic field on the separatrix in the regions $|Z| > \zeta^{1/2}$.

When combined with the rotamak condition of a rigid-body rotation of the electron fluid, the Ψ^2 model has a more realistic density distribution than that of the Solov'ev model, and is therefore more useful for the power balance calculations presented by DRC.

Acknowledgment

We thank Professor I. R. Jones who stimulated this work by suggesting that the energy loss processes in the rotamak configuration be analysed.

References

- Abramowitz, M., and Stegun, I. A. (1965). 'Handbook of Mathematical Functions' (Dover: New York).
- Berk, H. L., Hammer, J. H., and Weitzner, H. (1981). *Phys. Fluids* **24**, 1758.
- Donnelly, I. J., Rose, E. K., and Cook, J. L. (1987). Power balance models for rotamak plasmas. *Aust. J. Phys.* **40**, (in press).
- Durance, G., Hogg, G. R., Tendys, J., and Watterson, P. A. (1987). Studies of equilibrium in the AAEC rotamak. *Plasma Phys. Contr. Fusion* (in press).
- Durance, G., and Jones, I. R. (1986). *Phys. Fluids* **29**, 1196.
- Grimm, R. C., Greene, J. M., and Johnson, J. L. (1976). 'Methods in Computational Physics', Vol. 16 (Ed. J. Killeen), p. 253 (Academic: New York).
- Hugrass, W. N., Jones, I. R., McKenna, K. F., Phillips, M. G. R., Storer, R. G., and Tucek, H. (1980). *Phys. Rev. Lett.* **25**, 1676.
- Jones, I. R., and Hugrass, W. N. (1981). *J. Plasma Phys.* **26**, 441.
- Solov'ev, L. S. (1975). 'Reviews of Plasma Physics', Vol. 6 (Ed. M. A. Leonovich), p. 239 (Consultants Bureau: New York).
- Storer, R. G. (1982). *Plasma Phys.* **24**, 543.

Appendix. Solov'ev Model Equilibria

Analytic solutions of the Grad-Shafranov equation can be found when $P \propto \Psi$ (Solov'ev 1975). In this case, equation (1) is a linear inhomogeneous partial differential equation. With the notation defined in Sections 2 and 3, the following relations hold:

$$\psi(X, Z) = 4X^2\{1 - X^2 - (Z/\zeta)^2\}, \quad \psi_0 = \left(\frac{\mu_0 \zeta^2 R^4 P_0}{8(4\zeta^2 + 1)}\right)^{\frac{1}{2}}, \quad (\text{A1})$$

$$J_\phi = \frac{8(4\zeta^2 + 1)\psi_0}{\mu_0 \zeta^2 R^3} X, \quad I_\phi = \frac{16(4\zeta^2 + 1)\psi_0}{3\mu_0 \zeta R}, \quad (\text{A2})$$

$$B_r = \frac{8\psi_0}{\zeta^2 R^2} XZ, \quad B_z = \frac{8\psi_0}{R^2} \{1 - 2X^2 - (Z/\zeta)^2\}. \quad (\text{A3})$$

Manuscript received 12 May, accepted 15 October 1986

